Available online at www.sciencedirect.com

ScienceDirect

Energy Procedia 59 (2014) 75 – 81

Energy Procedia

European Geosciences Union General Assembly 2014, EGU 2014

# Experimental rig to improve the geophysical and geomechanical understanding of $CO_2$ reservoirs

Ismael Falcon-Suarez[a,]*, Laurence North[a], Angus Best[a]

[a]National Oceanography Centre, University of Southampton Waterfront Campus, Southampton, United Kingdom

**Abstract**

We intend to perform experiments that simulate real Carbon Capture and Storage (CCS) conditions in the laboratory, and hence provide the necessary knowledge to interpret field seismic surveys. Primarily, our research is focused on determining seismic rock properties (i.e., wave velocities and attenuation) of real and artificial 50 mm diameter brine-$CO_2$-bearing sandstone and sand samples that are representative host rocks of real CCS scenarios. Accordingly, we have integrated into a new triaxial cell system both an ultrasonic pulse-echo method for accurate velocity (± 0.3%) and attenuation (± 0.1 dB $cm^{-1}$) measurements, and an electrical resistivity tomography (ERT) method to monitor homogeneity of pore fluid distribution within the samples. The use of ERT provides calibration data for field scale techniques (such as marine controlled source electromagnetic surveying) but also allows measurements of bulk resistivity, fluid diffusion monitoring, flow pathway characterization, and determination of the relative permeability for different brine/brine-$CO_2$ ratios. By simultaneously measuring ultrasonic P- and S-wave velocities and electrical resistivity, we also provide data for joint inversion of seismic and electric field data. Furthermore, the stress-strain behaviour of the sample is continuously monitored with the aid of electrical gauges, so that we deal consistently and simultaneously with the geophysical and geomechanical response of the reservoir when submitted to $CO_2$ injections.


Peer-review under responsibility of the Austrian Academy of Sciences

*Keywords:* CCS; experimental rig; acoustic properties; electrical resistivity; stress-strain; permeability

* Corresponding author. Tel.: +44 (0)2380-56666; fax: +44 (0)2380-635130.
*E-mail address:* isfalc@noc.ac.uk


Peer-review under responsibility of the Austrian Academy of Sciences
doi:10.1016/j.egypro.2014.10.351

## 1. Introduction

The capture of Carbon Dioxide ($CO_2$) from stationary sources and injection of $CO_2$ into deep geological formations through boreholes (Carbon Capture and Storage - CCS) is a possible technological, global scale solution to mitigate against rising levels of atmospheric greenhouse gases. Reservoir rock stability during injection is typically monitored with time-lapse (4D) seismic surveying tools, which could help to discriminate between fluid pressure and fluid saturation changes.

$CO_2$ is a reactive fluid whether in a liquid, gas or supercritical state. When injected into deep geological formations it triggers various phenomena in porous media as a result of pressure and temperature gradients, and chemical disequilibria [1]. The need to accurately model these phenomena using 3D earth models of storage sites constrained by field and laboratory data has been specified in legislation, for example European Directive 2009/31/EC. The constraining data required for 3D earth models include host rock pore volume, $CO_2$–rock geochemical reactions, geomechanical behavior of the seal and reservoir, and fluid flow dynamics. All of these parameters are interconnected and can be grouped under the term "Thermo-Hydro-Mechano-Chemical" coupled processes (THMCs).

Typically, flooding tests with supercritical $CO_2$ in the laboratory are performed on experimental rigs specially designed for conducting flow through porous media at high pressure. Design of the rig is far from trivial and must be optimized to meet the requirements of each simulating scenario: the accurate control of pore fluid, confining pressure, temperature and flow, and integrated monitoring tools is essential [2]. Therefore, to address the study of THMCs, at the National Oceanography Centre (NOC), we are developing an experimental rig to perform $scCO_2$ injection tests while simultaneously monitoring physical and hydromechanical properties of the reservoir formations under in situ conditions.

**Nomenclature**

| | |
|---|---|
| CCS | Carbon Capture and Storage |
| THMCs | Thermo-Hydro-Mechano-Chemical coupled processes |
| ERT | Resistivity Tomography Measurements |
| FTV | Fluid Transfer Vessel |
| $ScCO_2$ | Supercritical $CO_2$ |
| $\sigma_{1=2=3}$ | Hydrostatic conditions of confining pressure |
| Pp | Pore pressure |
| $V_P$ | P-wave velocity |
| $Q_P^{-1}$ | P-wave attenuation |
| $\sigma_{cc}$ | initial crack closure |
| $\sigma_{ci}$ | linear elastic |
| $\sigma_{cd}$ | crack growth |
| $\sigma_{UCS}$ | unstable crack growth |

## 2. Experimental Rig

The experimental rig developed in the rock physics laboratory at the NOC aims to simulate real conditions of injection that take place during CCS activities (Fig. 1). The rig integrates (i) controllers, (ii) a triaxial cell core holder, (iii) data loggers, and (iv) hydraulic accessories.

### *2.1. Controllers*

The controllers allow the accurate manipulation of environmental conditions of the experiment, i.e., temperature and pressure. At present, the confining pressure is set by manual ENERPAC pumps; the pore pressure is controlled by an electronic SCO DX100 pumping controller (up to 69 MPa). This system allows highly accurate monitoring of pressure, flow rates and cumulative volumes.

Temperature is set by using a dual thermocouple-DEHS (Digital Electric Heating System) configuration. The whole system is wrapped with a rope heater so that the temperature of injected fluid and the oil inside the triaxial vessel can be controlled.

### *2.2. Triaxial cell core holder*

The core holder used is a modified Hoek-Franklin type. The rubber sleeve that isolates the core plug from the confining fluid (Fig. 2) is equipped with 16 electrodes for electrical resistivity tomography measurements (ERT), as described in [3]. Strain gauges (350 Ohm) can be added either on the sleeve or the sample to accurately measure axial and lateral strains. Note that if added on the sleeve, calibration with standard materials is required. The strain gauge wires exit the triaxial cell through paths on the in- and out-let load platens. In addition, the platens have been specifically designed to accommodate transducers that are in direct contact with acrylic buffer roads, which are likewise in contact with the sample. The buffer rods isolate the sample from the rest of the rig and provide and acoustic delay between the ultrasonic transducer and sample. The delay provided by the buffer rods (of well-defined acoustic impedance and low loss) enables the identification of top/base sample reflections for calculating velocity and attenuation using a pulse-echo method [4]. The buffer rods and the platens are also drilled to provide pathways (in- and out-let ports) to conduct pore fluid through the sample.

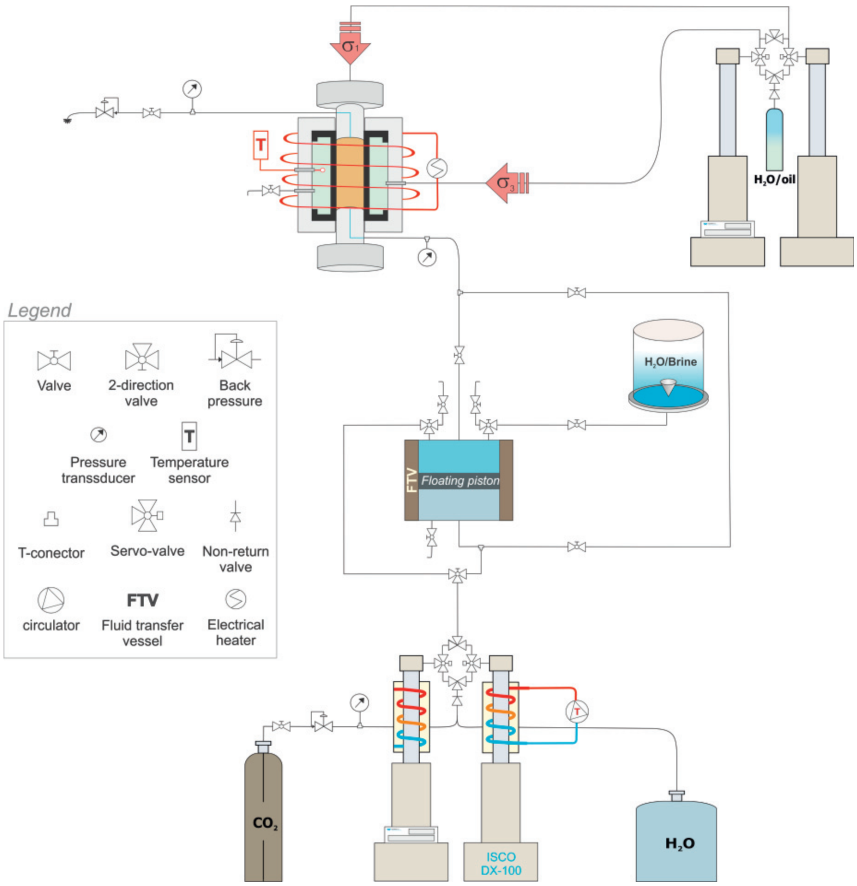


Fig. 1. Experimental rig for simulating $CO_2$ injections concerning CCS activities [2].

### 2.3. Data loggers

In addition to the controllers, each instrument is provided with its own data logger. The ultrasonic pulse-echo instrumentation measures the ultrasonic velocity to a precision of ± 0.3% and the ultrasonic attenuation to a precision of ± 0.1 dB $cm^{-1}$ [5]. The ERT bases on a typical tetra-polar electrode configuration Electric Impedance Tomography measurement system [3]. The configuration of the 16 electrode array allows us to obtain a total of 208 measurements. The electrical strain gauges are connected to a Micro-measurements D4 (Vishay Precision Group®) data acquisition conditioner, with a sampling rate of up to 8 Hz. Beside the geophysical and geomechanical instrumentation, to further control the pore pressure in our experimental rig four piezoresistive pressure transmitters (Keller-druck®) are implemented in the hydraulic system (described below) to accurately measure pressure but also temperature changes in the injected fluid with a frequency up to 2 Hz.

### 2.4. Hydraulic accessories

The hydraulic system is composed of a high pressure network of pipes, valves, connectors, backpressures and other accessories (Swagelok®) to satisfy different experimental configurations). Pore fluid is injected from a fluid transfer vessel (FTV), which acts as an intermediate flow transmitter that isolates the corrosive fluids (brine, brine+$CO_2$) from the pumping controller, preventing potential damage to the ISCO accessories. The piezoresistive pressure transmitters are emplaced in the FTV, and other key positions within the hydraulic circuit to provide accurate monitoring of pressure at key points within the circuit, for instance those placed up- and down-stream of the sample which can be used for determining permeability.

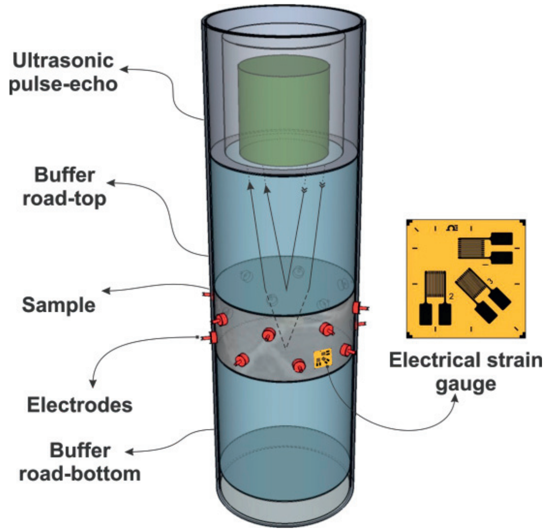


Fig. 2. Drawing of the sleeve within the triaxial cell [2].

## 3. Rig calibration: Preliminary results

The experimental rig is currently still in development. So far, acoustic measurements have been successfully performed. We have used sandstone of well-known properties to test both tools. Table 1 shows some main properties of the sample. The mineralogy was determined from XRD analysis for each rock type. Petrographic analysis revealed the presence of trace amounts of detrital minerals that included feldspas, biotite mica and clays. On the other hand, porosity and permeability were calculated experimentally: the first by helium porosimetry for total porosity, and via saturated-dried weight-difference for effective porosity; the second, forcing steady state conditions (i.e., Darcy's law). The saturation process was carried out via imbibition vacuum-forced.

Table 1. Properties of tested sandstone.

| Sample properties | Value | Unit |
|---|---|---|
| Length | 0.02 | m |
| Diameter | 0.05 | m |
| Bulk density | 2400 | kg $m^{-3}$ |
| Porosity | 0.15 | $m^3$ $m^{-3}$ |
| Permeability | ~$10^{-15}$ | $m^2$ |
| Mineralogy | Quarz (98), Clay+Fds+Bio (<1.5) | % |

After saturation with brine of density ~1030 g $dm^{-3}$ (i.e., see water) the sample was placed in the triaxial cell and pressurized under hydrostatic confining conditions (i.e., $\sigma_{1=2=3}$) of 18 MPa, while pore pressure (Pp) was set at 7 MPa (i.e., 11 MPa of effective pressure). Then the same brine as that used for saturating the sample was forced through the sample. The total volume of brine forced through the sample was approximately eight times the pore volume. After measuring the geophysical properties with pure brine, the brine was partially saturated with $CO_2$ and same procedure was carried out (i.e., the mixture flow through the sample until original brine was replaced).

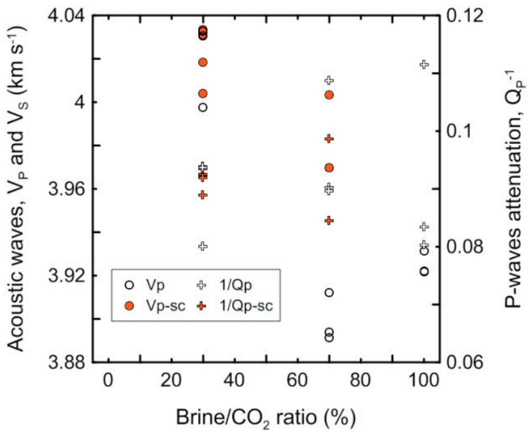


Fig. 3. P-wave velocity and attenuation of sandstone sample at different brine to $CO_2$ ratio, hydrostatic confining pressure and pore pressure and temperature around the $CO_2$ supercritical point (7.3 MPa, 31.1 ºC).

Fig. 3 shows P-waves velocity ($V_P$) and attenuation ($Q_P^{-1}$) preliminary results for different brine to $CO_2$ ratios regarding the first test carried out with the sandstone sample described above (Table 1). Measurements were performed around the supercritical point of $CO_2$, increasing both the confining and pore pressure so that effective pressure remained constant (i.e., $\sigma_{1=2=3}$=19 MPa, Pp=8 MPa and 38 ºC).

## 4. Ongoing work and expected results

### *4.1. Geophysical and hydromechacnical information*

Acoustic waves can provide information about the physical properties of porous media. Changes in the attenuation and velocity of elastic waves are a function of both the pore network and the pore fluid (see Fig. 4a or

Fig. 3) and also the confining pressure (Fig. 4b). Because the pore fluid and confining pressure are controlled variables in our system, we are able to determine changes in the stress-strain state of the rock during our experiments. Furthermore, an overview of a typical stress-strain evolution in sandstone (Fig. 4c) shows different strain stages during loading (initial crack closure, $\sigma_{cc}$; linear elastic, $\sigma_{ci}$; crack growth, $\sigma_{cd}$; and unstable crack growth, $\sigma_{UCS}$).

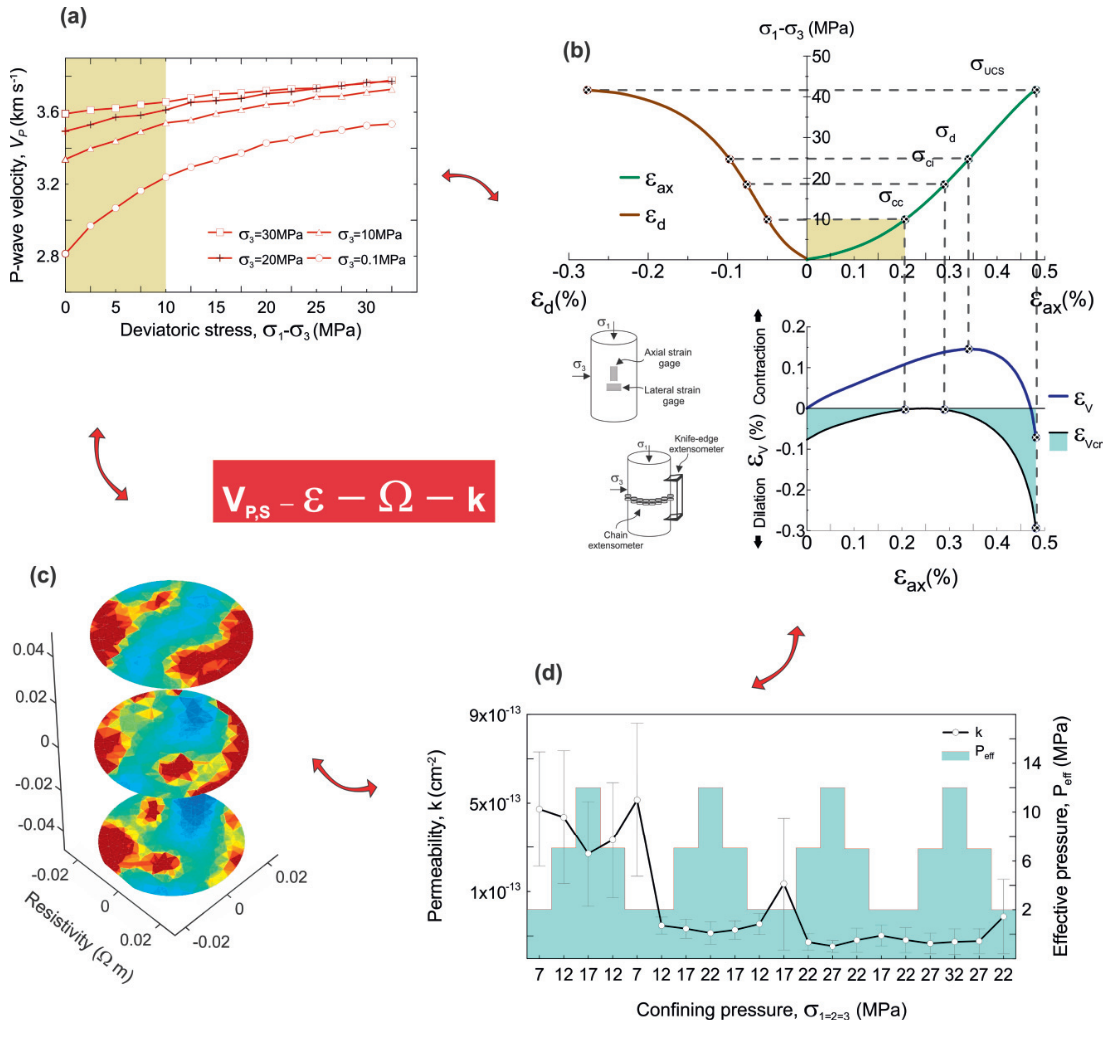


Fig. 4. Example of interaction between THMC phenomena: (a) evolution of P-wave velocity by increasing the deviatoric stress; (b) typical stress-strain diagram of a Corvio sandstone [2]; (c) anisotropic electrical resistivity measurement [3]; (d) permeability variations with changes in effective and/or confining pressure.

The mechanical behavior is expected to be different from one strain stress state to other. Indeed, the acoustic wave diagram for the same example (comparison between Fig. 4b and Fig. 4c) demonstrates that, at low axial pressure and below 10 MPa deviator stress, P-wave velocities show a non-linear evolution (dark yellow square), which agrees with the first stress-strain stage ($\sigma_{cc}$). Hence, neglecting the initial state of stress may lead to incorrect data interpretation.

Electrical resistivity (Fig. 4d) can be used to monitor fluid pathways and compositional changes in the pore solution (e.g. $CO_2$ replacing brine). It offers valuable information about progressive stages of partial saturation that can be easily converted into relative permeability (Fig. 4e) by controlling the pore pressure and water flow (Darcy's law). So, acoustic wave velocities and attenuations, electrical resistivity, stress-strain evolution and permeability can be simultaneously monitoring, reporting multidisciplinary information regarding the phenomena that occur in the porous media as a result of varying the original conditions.

### *4.2. Geochemical and mineralogical analysis*

Neglecting geochemical aspects can lead to wrong interpretation of experimental results. Therefore, as a part of the test is worth monitoring outflow pore water in terms of electrical conductivity and pH, and also chemical composition. This aids the recognition of geochemical changes associated with each stage of the experiment [1]. The analysis of mineralogical changes by sample comparison before and after testing, and variations in the pore size distribution, if any, is also interesting to properly understand the geochemical evolution of the system.

As a final step, all data obtained during the test can be integrated and analyzed together around the THMCs concept. With this new experimental design, we will be able to establish cause-consequence sequences, and the relevance of each parameter within the reservoir complex, at the prescribed experimental conditions.

## Acknowledgements

This work is a part of the UK EPSRC DiSECCS project, and contains data obtained during the stay of I. Falcon Suarez at the facilities of LAMEROC (University of A Coruña) under the supervision of Professor Jordi Delgado Martin.

## References

[1] Canal J, Delgado J, Falcón I, Yang Q, Juncosa R, Barrientos V. Injection of $CO_2$-Saturated Water through a Siliceous Sandstone Plug from the Hontomin Test Site (Spain): Experiment and Modelling. *Env Sci Tech* 2013;47(1):159-67.

[2] Falcon-Suarez I, North L, Best AI, Sothcott J, Canal-Vila J, Delgado-Martin J. Laboratory simulation of $CO_2$ injection in sandstones and sands for improved seismic monitoring of $CO_2$ reservoirs. *Rock Eng Rock Mech: Structures in and on Rock Masses*: CRC Press; 2014. p. 1301-4.

[3] North L, Best AI, Sothcott J, MacGregor L. Laboratory determination of the full electrical resistivity tensor of heterogeneous carbonate rocks at elevated pressures. *Geophys Prospect* 2013;61(2):458-70.

[4] Best AI, McCann C, Sothcott J. The relationships between the velocities, attenuations and petrophysical properties of reservoir sedimentary rocks1. *Geophys Prospect* 1994;42(2):151-78.

[5] Best AI, Sothcott J, McCann C. A laboratory study of seismic velocity and attenuation anisotropy in near-surface sedimentary rocks. *Geophys Prospect* 2007;55(5):609-25.